
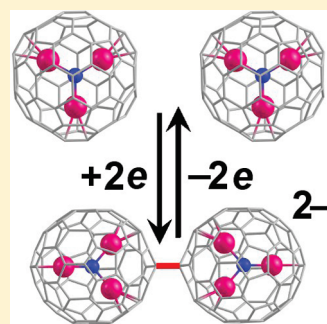


Dimerization of Radical-Anions: Nitride Clusterfullerenes versus Empty Fullerenes

Alexey A. Popov,^{*,†,‡} Stanislav M. Avdoshenko,[§] Gianaurelio Cuniberti,^{§,||} and Lothar Dunsch[†][†]Department of Electrochemistry and Conducting Polymers, The Center of Spectroelectrochemistry, Leibniz Institute of Solid State and Materials Research (IFW) Dresden, Helmholtzstr. 20, D-01069 Dresden, Germany[‡]Chemistry Department, Moscow State University, 119992 Moscow, Russian Federation[§]Institute for Materials Science and Max Bergmann Center of Biomaterials, Dresden University of Technology, D-01062 Dresden, Germany^{||}Division of IT Convergence Engineering and National Center for Nanomaterials Technology, POSTECH, Pohang 790-784, Republic of Korea Supporting Information

ABSTRACT: In contrast with empty fullerenes, nitride clusterfullerenes usually exhibit irreversible reduction steps at moderate electrochemical scan rates. However, these reduction steps are chemically reversible, indicating that reversible follow-up reaction takes place. To explain this phenomenon, we analyze in this work if anion-radicals of nitride clusterfullerenes are more prone to dimerization than anion-radicals of empty fullerenes. Extensive DFT computations are performed to find the most stable dianionic dimeric structures of $\text{Sc}_3\text{N@C}_{68}$, $\text{Sc}_3\text{N@C}_{80}$, $\text{Sc}_3\text{N@C}_{80}(\text{CF}_3)_2$, [5,6] and [6,6] pyrrolidine adducts of $\text{Sc}_3\text{N@C}_{80}$ and $\text{Y}_3\text{N@C}_{80}$, a series of $\text{Y}_3\text{N@C}_{2n}$ ($2n = 78, 80, 84, 86, 88$), as well as those of empty fullerenes C_{60} , C_{70} , and C_{84} . Dimerization energies of the most stable isomers are computed in the gas phase, with the use of van der Waals corrections, and in solution. It is found that dianionic dimers of nonderivatized nitride clusterfullerenes are substantially more stable than those of empty fullerenes, which can be an explanation of the electrochemical irreversibility of the former.

SECTION: Molecular Structure, Quantum Chemistry, General Theory



One of the important properties of fullerenes for their broad applications is the ease with which they can accept electrons. Endohedral metallofullerenes, and, in particular, nitride clusterfullerenes (NCFs) also exhibit such properties^{1–3} (gas-phase electron affinity of $\text{Sc}_3\text{N@C}_{80}$ is even higher than that of C_{60} ⁴). Moreover, in a number of recent studies, NCFs have been shown to be superior to C_{60} in photovoltaic applications.^{5–8} Despite the importance of the electron transfer reactions of NCFs in this context, there is still a challenging question that has not been clearly understood up to now. Whereas empty fullerenes exhibit perfectly reversible reduction steps in solution at room temperature, the majority of NCFs exhibit irreversible reduction behavior at standard voltammetric scan rates.^{9–17} For $\text{Sc}_3\text{N@C}_{80}$, Echegoyen has shown that electrochemical reversibility can be reached at fast scan rates (5 V/s was reported for the first reduction step).⁹ Extended studies of $\text{Dy}_3\text{N@C}_{78}$ and $\text{Dy}_3\text{N@C}_{80}$ have shown that for these NCFs electrochemically reversible reductions were not achieved up to the scan rates of 80 V/s.¹⁴ Likewise, irreversible reduction steps are also observed for $\text{Sc}_3\text{N@C}_{68}$,¹⁵ $\text{Sc}_3\text{N@C}_{78}$,¹⁸ and a series of $\text{M}_3\text{N@C}_{2n}$ ($\text{M} = \text{lanthanide}$),² the only exclusion from this rule being $\text{M}_3\text{N@C}_{88}$, which exhibited reversible reductions.¹⁷ Dedicated studies have shown that despite electrochemical irreversibility, reduction

steps of NCFs are chemically reversible.^{9,10,14} That is, the follow-up reaction accompanying electron transfer is reversible and pristine NCFs can be recovered at the end of a voltammetric cycle. Thus, irreversible reactions with the solvent and the sample decomposition can be excluded. (This was shown by multiple cycling as well as mass-spectrometric studies of the electrolysis products, which showed no traces of NCFs' derivatives.) To explain this peculiar reduction behavior of NCFs, we suggested a double-square schema in which structural rearrangement of the cluster (e.g., pyramidalization) in radical anions was proposed;^{14,16} however, the nature of this rearrangement remained unclear. Extended theoretical studies of the charged NCFs did not reveal any structural changes that might be responsible for the irreversibility of electrochemical reduction.^{19–22}

Chemical derivatization of NCFs also changes their electrochemical properties. It was shown that trifluoromethylated $\text{Sc}_3\text{N@C}_{80}$ derivatives tend to exhibit electrochemically reversible reduction steps. For $\text{Sc}_3\text{N@C}_{80}(\text{CF}_3)_2$, three reversible reduction steps have been observed, and stability of the radical

Received: May 2, 2011

Accepted: June 7, 2011

anion and trianion was sufficient to afford their characterization by ESR spectroscopy.²³ Likewise, [5,6] cycloadducts of $\text{Sc}_3\text{N}@C_{80}$ and $\text{Y}_3\text{N}@C_{80}$ also exhibit reversible reduction steps.² For a [5,6] pyrrolidine adducts of $\text{Y}_3\text{N}@C_{80}$, Echegoyen et al. have succeeded in characterization of the anion-radical by ESR spectroscopy.²⁴ At the same time, detection of $\text{Y}_3\text{N}@C_{80}^-$ anion-radical by in situ ESR spectroelectrochemistry was not possible, showing that diamagnetic product is formed upon reduction.¹⁶ In contrast with [5,6] adducts, [6,6] adducts of $\text{M}_3\text{N}@C_{80}$ ($\text{M} = \text{Er}, \text{Y}, \text{Lu}$) usually show irreversible behavior similar to the respective underivatized NCFs.^{10,25} However, recently, the first examples of [6,6]-adducts of $\text{Sc}_3\text{N}@C_{80}$ with reversible reductions were reported.^{25,26}

A possible explanation of the reduction behavior of NCFs was proposed in our in situ ESR/vis-NIR spectroelectrochemical study of $\text{Sc}_3\text{N}@C_{68}$.¹⁵ $\text{Sc}_3\text{N}@C_{68}$ exhibits a reversible oxidation step that facilitated detection of its cation-radical by ESR spectroscopy. We have also succeeded in detecting the ESR spectrum of the anion-radical under the same experimental condition, but the spin number obtained via integrated intensity of $\text{Sc}_3\text{N}@C_{68}^-$ ESR signal was almost an order of magnitude lower than that of the cation-radical despite the same currents (i.e., the same number of transferred electrons). This indicated that in addition to the anion-radical, an electron transfer to $\text{Sc}_3\text{N}@C_{68}$ also results in the reversible formation of the diamagnetic compound, and dimerization of $\text{Sc}_3\text{N}@C_{68}^-$ with formation of the single-bonded dianionic dimer was proposed. It should be noted that formation of such dimers is known for empty fullerenes in the solid phase but has never been observed in solution.^{27,28} In this work, we use an extended DFT study to analyze if dimerization of anion-radicals can be responsible for the irreversible reduction behavior of NCFs.

Search for Stable Isomers of Fullerene Dimer. Complete understanding of the mechanisms of the follow-up reaction at the electrode requires clarification of the interplay between kinetic and thermodynamic factors. In this work, we consider only the thermodynamic factor; in particular, we analyze which component should prevail in solution if an equilibrium is established in the reaction $2(\text{FLRN})^- \leftrightarrow (\text{FLRN})_2^{2-}$, where FLRN stands for any fullerene structure. For all fullerenes larger than C_{60} , at least two different kinds of carbon atoms are available in the carbon cage, thus leading to the multiple possible inter cage links in corresponding dianionic dimers. In endohedral metallofullerenes, the situation is additionally complicated by a possibility of different positions for endohedral metal atoms. Thus, in the first stage of this study, it is necessary to find the most stable dimers among many possible isomers for all fullerene structures under consideration. Taking into account the relatively low symmetry of many NCFs, this leads to many tens of possible isomers, which makes complete DFT study hardly feasible in this stage. In a series of testing calculations (Supporting Information), we have found that relative energies of $(\text{FLRN})_2^{2-}$ isomers correlate very well with the relative energies of $(\text{FLRN})\text{CH}_3^-$ isomers. (Importantly, the slope of the linear correlation between relative energies is close to 2, pointing to additive contributions of each monomeric unit.) Besides, monomeric fullerene fragments from the optimized $(\text{FLRN})\text{CH}_3^-$ structures form very good structural guess for $(\text{FLRN})_2^{2-}$ dimers, and optimization of the latter then converges rapidly. These facts dramatically facilitate the search of the stable isomers of the dimers because computational demands can be reduced drastically. Thus, for each fullerene discussed below, the following multistep algorithm was adopted:

first, we have optimized many $(\text{FLRN})\text{CH}_3^-$ isomers (up to 80 isomers were considered for some NCFs) at the PBE/DZ(P) level (DZ(P) abbreviation here stands for the DZ-quality basis set for carbon atoms and DZVP-quality basis for endohedral nitrogen, scandium, and yttrium atoms); then, $(\text{FLRN})_2^{2-}$ isomers were optimized at the PBE/DZ(P) level for the 5–15 lowest energy $(\text{FLRN})\text{CH}_3^-$ isomers. (The number of considered isomers depends on the density of relative energy distribution.) In the final stage, one to five of the most stable isomers of the dimers were reoptimized at the PBE/TZ2P level of theory. Dimers were studied in their singlet states, which is justified by their relatively high HOMO–LUMO gaps (>0.5 eV in most cases; testing calculations have also shown that triplet states of dimerized $\text{Sc}_3\text{N}@C_{68}^-$, $\text{Sc}_3\text{N}@C_{80}^-$, and $\text{Y}_3\text{N}@C_{80}^-$ are ca. 100 kJ/mol less stable than respective singlet states). The use of this multistep algorithm ensures that the most stable isomers of the dimeric structures are located for each fullerene structure with high degree of certainty. It should be noted that the “mixed” asymmetric dimers (i.e., those in which monomeric units are bonded through different kinds of carbon atoms) were not considered in this work because our preliminary studies have shown that relative energies of such dimers can be roughly computed as the mean value of corresponding symmetric dimers. Besides, conformers obtained by rotation around the FLRN–FLRN bond were not considered in detail because preliminary studies have shown that relative energies of different conformers are usually within 1 to 2 kJ/mol.

Dimers of Empty Fullerenes. Dianionic single-bonded dimers of C_{60} and C_{70} (Figure 1a) have been previously characterized in detail both experimentally and computationally. (For a recent extended computational study, see ref 29 and references therein.) Note that both $(C_{60})_2^{2-}$ and $(C_{70})_2^{2-}$ are available in the solid phase, and the molecular structure of the experimentally characterized $(C_{70})_2^{2-}$ corresponds to the most stable isomer of $(C_{70})_2^{2-}$ predicted by calculations. Because the size of the fullerene can influence the dimerization energy (for instance, because of the different on-site Coulomb repulsion between charged monomeric units), in this work, we have also studied the isomers of $(C_{84}-D_{2d}(23))_2^{2-}$. From 11 symmetry nonequivalent atoms of $C_{84}-D_{2d}(23)$, three are located on triple hexagon junctions (THJs), and corresponding $(C_{84}-D_{2d}(23))\text{CH}_3^-$ isomers are very unstable, which agrees with the general trend in addition chemistry of higher fullerenes to avoid THJs. Among the remaining eight carbon atoms, four provide almost isoenergetic $(C_{84})_2^{2-}$ dimers (relative energies within 5 kJ/mol at the PBE/TZ2P level), of which the two most stable ones are shown in Figure 1b. Similar to C_{70}^- ,²⁹ the stability of $(C_{84})_2^{2-}$ isomers roughly correlates with POAV angles of C_{84}^- .

Dimers of $\text{Sc}_3\text{N}@C_{68}$, $\text{Sc}_3\text{N}@C_{80}$, and Its Derivatives. Dimers of $\text{Sc}_3\text{N}@C_{68}^-$ were previously studied by us.¹⁵ In brief, the most stable dimeric structures (Figure 1c) are bonded via peripheral carbon atoms of the pentalene unit. Chemical activity of the atoms in adjacent pentagons was previously shown for $\text{M}_2@C_{72}$ as well as for $\text{Sc}_3\text{N}@C_{68}$.^{30–32}

Our previous studies of $(\text{Sc}_3\text{N}@C_{80}-I_h)^-$ have shown two conformers of the anion, with C_{3v} and C_s symmetries, are especially stable.¹⁹ (In the following, we will consider only the $I_h(7)$ cage isomer of C_{80} , and hence designation of the carbon cage isomers will be avoided hereafter.) At a starting point, we have studied $\text{Sc}_3\text{N}@C_{80}(\text{CH}_3)^-$ isomers arising from the addition of CH_3 groups to all symmetry nonequivalent carbon atoms of both conformers (62 isomers totally). Optimization resulted

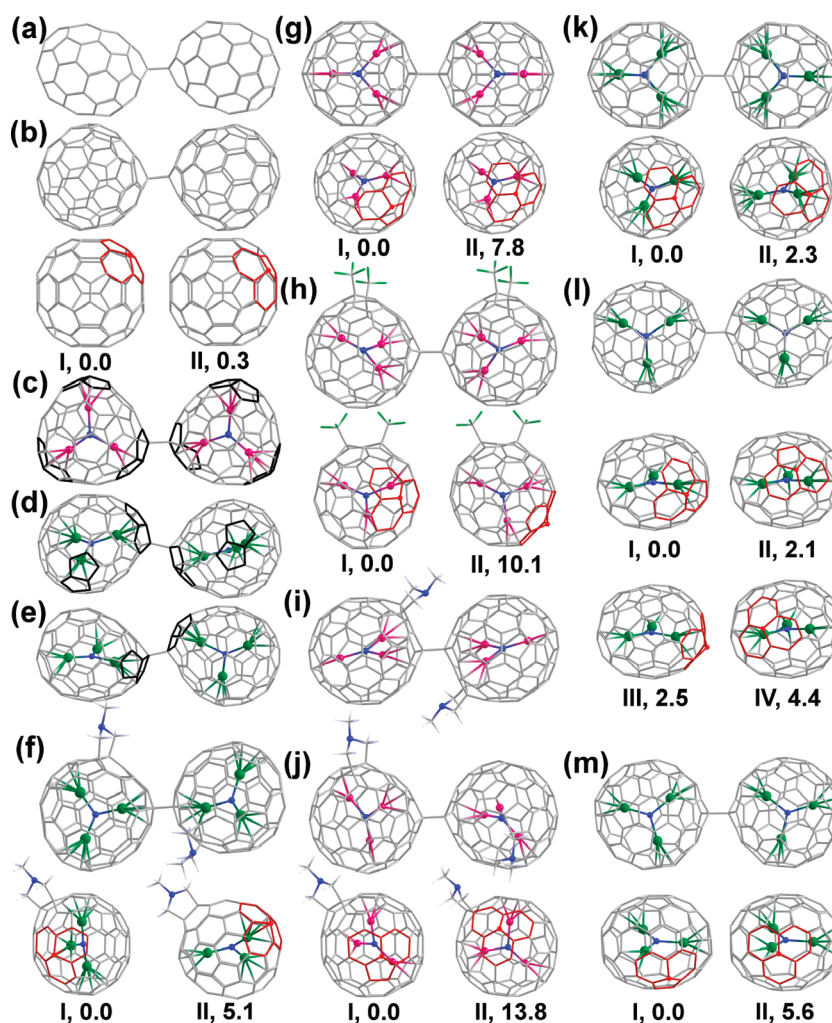


Figure 1. Molecular structures of the lowest energy isomers of $(\text{FLRN})_2^{2-}$: (a) $(\text{C}_{70})_2^{2-}$, (b) $(\text{C}_{84}\text{-D}_{2d}(23))_2^{2-}$, (c) $(\text{Sc}_3\text{N@C}_{68})_2^{2-}$, (d) $(\text{Y}_3\text{N@C}_{78})_2^{2-}$, (e) $(\text{Y}_3\text{N@C}_{84})_2^{2-}$, (f) $([\text{6,6}]\text{-Y}_3\text{N@C}_{80}(\text{C}_3\text{H}_7\text{N}))_2^{2-}$, (g) $(\text{Sc}_3\text{N@C}_{80})_2^{2-}$, (h) $(\text{Sc}_3\text{N@C}_{80}(\text{CF}_3)_2)_2^{2-}$, (i) $([\text{5,6}]\text{-Sc}_3\text{N@C}_{80}(\text{C}_3\text{H}_7\text{N}))_2^{2-}$, (j) $([\text{6,6}]\text{-Sc}_3\text{N@C}_{80}(\text{C}_3\text{H}_7\text{N}))_2^{2-}$, (k) $(\text{Y}_3\text{N@C}_{80})_2^{2-}$, (l) $(\text{Y}_3\text{N@C}_{86})_2^{2-}$, and (m) $(\text{Y}_3\text{N@C}_{88})_2^{2-}$. Carbon atoms are gray except for adjacent pentagon pairs, which are highlighted in black; nitrogen atoms are blue; Sc, magenta; Y, green. If two or more stable isomers are found, then their numbers, relative energies (gas phase, kJ/mol at the PBE/TZ2P level), and monomeric fragments are shown with the intercage bonding site and adjacent rings highlighted in red.

in a smaller number of nonequivalent $\text{Sc}_3\text{N@C}_{80}(\text{CH}_3)^-$ isomers because in some cases the cluster rotated during optimization procedure. Eight most stable structures were then chosen for dimerization studies, and two most stable $(\text{Sc}_3\text{N@C}_{80})_2^{2-}$ isomers are shown in Figure 1g. (All other isomers are at least 25 kJ/mol less stable at the PBE/DZ(P) level of theory.)

The structures of the two most stable isomers of $(\text{Sc}_3\text{N@C}_{80})_2^{2-}$ are closely related. They both have C_s -symmetric arrangement of the Sc_3N cluster inside the cage, whereas carbon atoms forming the intercage bond are located near the plane of the cluster and between the coordination sites of two equivalent Sc atoms. The only difference between two isomers is that the most stable structure is bonded via carbon atoms on the pentagon–hexagon–hexagon junction (PHHJ), whereas the slightly less stable isomer ($\Delta E = 7.8$ kJ/mol at PBE/TZ2P level) is bonded via the neighboring THJ atom. Interestingly, in contrast with empty fullerenes,³⁵ functionalization of $\text{Sc}_3\text{N@C}_{80}$ via THJ cage atoms does not lead to considerable destabilization of thus formed derivatives. (This finding agrees with the reported studies of the trifluoromethylation of $\text{Sc}_3\text{N@C}_{80}$.^{34,35})

In the previous studies of $\text{Sc}_3\text{N@C}_{80}(\text{CF}_3)_2$, we have found that the most stable structure has *para*- $\text{C}_6(\text{CF}_3)_2$ hexagon on one pole (both CF_3 groups are bonded to PHHJs) and the Sc_3N cluster located in such a way that one Sc atom is facing the cage hexagon on the opposite pole, whereas two other Sc atoms are coordinated close to the *para*-position of CF_3 -bearing carbon atoms.^{35,36} Considering the idealized C_2 symmetry of this conformer (in the actual optimized structure C_2 symmetry is slightly distorted), we have studied 39 isomers of $\text{Sc}_3\text{N@C}_{80}(\text{CF}_3)_2(\text{CH}_3)^-$.

The most stable isomer of $\text{Sc}_3\text{N@C}_{80}(\text{CF}_3)_2(\text{CH}_3)^-$ (30 kJ/mol lower in energy than all other isomers at PBE/DZ(P) level) has a CH_3 group attached to the PHHJ carbon atom in $\text{C}_6(\text{CF}_3)_2$ hexagon next to the CF_3 -bearing carbon atom. The use of this bonding site for dimerization is hardly possible for the obvious steric reasons, and our attempts to optimize such a dimer always resulted in the nonbonded state. The second most stable isomer of $\text{Sc}_3\text{N@C}_{80}(\text{CF}_3)_2(\text{CH}_3)^-$ ($\Delta E = 30$ kJ/mol at the PBE/DZ(P) level) also has its CH_3 group attached in the vicinity of

CF₃ groups. As a result, the corresponding dimer is highly strained ($\Delta E = 86$ kJ/mol at the PBE/DZ(P) level) and is not found among the stable isomers of $(\text{Sc}_3\text{N}@\text{C}_{80}(\text{CF}_3)_2)^{2-}$. The most stable isomer of $(\text{Sc}_3\text{N}@\text{C}_{80}(\text{CF}_3)_2)^{2-}$ thus corresponds only to the fourth most stable isomer of $\text{Sc}_3\text{N}@\text{C}_{80}(\text{CF}_3)_2^{2-}(\text{CH}_3)^-$ and is followed by two other isomers with close energies; in all three structures, binding sites are far away from CF₃ groups. Similar to $\text{Sc}_3\text{N}@\text{C}_{80}$, stable isomers are bonded through carbon atoms located between two Sc atoms close to the plane of the cluster (Figure 1h). Interestingly, the lowest energy isomer of $(\text{Sc}_3\text{N}@\text{C}_{80}(\text{CF}_3)_2)^{2-}$ is bonded via THJ, and the second most stable structure with PHHJ–PHHJ intercage bond is 10.1 kJ/mol less stable at the PBE/TZ2P level.

For [5,6] *N*-methyl pyrrolidine adduct $\text{Sc}_3\text{N}@\text{C}_{80}(\text{C}_3\text{H}_7\text{N})^-$, we have found that in the lowest energy location of the Sc_3N cluster its plane is parallel to the approximate plane of the pyrrolidine ring, and two Sc atoms are located close in para positions to C-sp³ atoms of the fullerene cage. In total, 45 isomers of $\text{Sc}_3\text{N}@\text{C}_{80}(\text{C}_3\text{H}_7\text{N})(\text{CH}_3)^-$ were considered corresponding to all nonequivalent cage carbon atoms in C_s-symmetric [5,6]- $\text{Sc}_3\text{N}@\text{C}_{80}(\text{C}_3\text{H}_7\text{N})$. The two most preferable isoenergetic CH₃-addition sites are found in $\text{Sc}_3\text{N}@\text{C}_{80}(\text{C}_3\text{H}_7\text{N})^-$: the first one is in the same pentagon, to which pyrrolidine moiety is already attached, and the second site is next to the first one on THJ. The most stable isomer of $([5,6]\text{-Sc}_3\text{N}@\text{C}_{80}(\text{C}_3\text{H}_7\text{N}))_2^{2-}$ corresponds to the second addition site, whereas the first one as well as the three other most stable isomers of $\text{Sc}_3\text{N}@\text{C}_{80}(\text{C}_3\text{H}_7\text{N})-(\text{CH}_3)^-$ with CH₃ group bonded close to the pyrrolidine moiety are sterically hindered for dimerization. As a result, the bonding state for such dimers is either not found or is highly strained. Therefore, the isomer of $([5,6]\text{-Sc}_3\text{N}@\text{C}_{80}(\text{C}_3\text{H}_7\text{N}))_2^{2-}$ shown in Figure 1i is at least 70 kJ/mol more stable than all other isomers at the PBE/DZ(P).

The situation with $[6,6]\text{-Sc}_3\text{N}@\text{C}_{80}(\text{C}_3\text{H}_7\text{N})^-$ is more complicated because the initial position of the cluster is not as well-defined as in the [5,6] isomer. In a preliminary study, we have found two stable conformers; in one of them the plane of the Sc_3N cluster is almost parallel to the approximate plane of the pyrrolidine ring, whereas in another conformer, it is perpendicular to the pyrrolidine ring. We optimized 43 and 42 isomers of $[6,6]\text{-Sc}_3\text{N}@\text{C}_{80}(\text{C}_3\text{H}_7\text{N})(\text{CH}_3)^-$ corresponding to each of the conformers, respectively, at the PBE/DZ(P) level, resulting in a total of 85 isomers. Similar to the [5,6] adduct, the most favorable CH₃ addition sites are located close to the pyrrolidine site, and corresponding dimers are highly strained. The most stable isomer of the dimer with its intercage bonding site located far from the pyrrolidine ring thus corresponds to the relatively unstable isomer of $[6,6]\text{-Sc}_3\text{N}@\text{C}_{80}(\text{C}_3\text{H}_7\text{N})(\text{CH}_3)^-$.

Dimers of $\text{Y}_3\text{N}@\text{C}_{2n}$ ($2n = 78, 80, 84, 86, 88$) and $\text{Y}_3\text{N}@\text{C}_{80}(\text{C}_3\text{H}_7\text{N})$ Nitride Clusterfullerenes. Non-IPR $\text{Y}_3\text{N}@\text{C}_{78}\text{--C}_{2-}$ (22010)³⁷ has 39 nonequivalent carbon atoms, all being subjected to CH₃ addition. Similar to the aforementioned $\text{Sc}_3\text{N}@\text{C}_{68}$, the most stable isomers of either $\text{Y}_3\text{N}@\text{C}_{78}(\text{CH}_3)^-$ or $(\text{Y}_3\text{N}@\text{C}_{78})_2^{2-}$ are bonded to peripheral atoms of adjacent pentagon pairs. The most stable isomer of $(\text{Y}_3\text{N}@\text{C}_{78})_2^{2-}$ shown in Figure 1e is at least 17 kJ/mol lower in energy than all other isomers at the PBE/DZ(P) level.

For $\text{Y}_3\text{N}@\text{C}_{80}\text{--I}_h(7)^-$, our previous studies have shown that two conformers, with C_s symmetry (analogues to that of $\text{Sc}_3\text{N}@\text{C}_{80}$) and with approximate D₃ symmetry (with Y atom facing the centers of hexagons), are the most stable ones.¹⁹ Consideration of all nonequivalent carbon atoms in these two conformers yields

58 isomers of $\text{Y}_3\text{N}@\text{C}_{80}(\text{CH}_3)^-$, all having been subjected to optimization at the PBE/DZ(P) level with subsequent optimization of 13 isomers of corresponding $(\text{Y}_3\text{N}@\text{C}_{80})_2^{2-}$ dimers. The two most stable isomers with relative energies of 0.0 and 2.3 kJ/mol at the PBE/TZ2P level are shown in Figure 1k. Importantly, the structure of the most stable isomer of $(\text{Y}_3\text{N}@\text{C}_{80})_2^{2-}$ corresponds to the second most stable isomers of $(\text{Sc}_3\text{N}@\text{C}_{80})_2^{2-}$ and is bonded via THJ carbon atoms; the second isomer of $(\text{Y}_3\text{N}@\text{C}_{80})_2^{2-}$ is noticeably different from that of $(\text{Sc}_3\text{N}@\text{C}_{80})_2^{2-}$: in the former, two monomeric units are bonded via THJ cage atoms, and one Y atom of each cluster is facing directly to the carbon atom participating in the intercage bond. This peculiar structure points to the strain experienced by the Y_3N cluster in relatively small C₈₀ cage, and coordination to the outward-pyramidalized carbon atom of the carbon cage allows partial release of this strain. Only the third most stable isomer of $(\text{Y}_3\text{N}@\text{C}_{80})_2^{2-}$ ($\Delta E = 24$ kJ/mol at the PBE/TZ2P level) is bonded via PHHJ atoms and is isostructural to the most stable isomer of $(\text{Sc}_3\text{N}@\text{C}_{80})_2^{2-}$ discussed above.

For the [5,6] and [6,6] isomers of $\text{Y}_3\text{N}@\text{C}_{80}(\text{C}_3\text{H}_7\text{N})$, we used the same starting coordinates as described above for $\text{Sc}_3\text{N}@\text{C}_{80}(\text{C}_3\text{H}_7\text{N})$ with Sc replaced by Y. The procedure has shown that the most stable isomer of $([5,6]\text{-Y}_3\text{N}@\text{C}_{80}(\text{C}_3\text{H}_7\text{N}))_2^{2-}$ is isostructural to the Sc counterpart. On the contrary, substantially different results from the Sc-based dimers were obtained for $([6,6]\text{-Y}_3\text{N}@\text{C}_{80}(\text{C}_3\text{H}_7\text{N}))_2^{2-}$. The intercage bonding patterns of the two most stable isomers of the latter are similar to that of $(\text{Y}_3\text{N}@\text{C}_{80})_2^{2-}\text{--II}$ with Y atom facing directly the THJ carbon atoms forming the intercage bond; the isomers isostructural to the most stable isomers of $([6,6]\text{-Sc}_3\text{N}@\text{C}_{80}(\text{C}_3\text{H}_7\text{N}))_2^{2-}$ are substantially higher in energy.

$\text{Y}_3\text{N}@\text{C}_{84}$ has non-IPR C_s(51365) carbon cage,^{38,39} but the Y_3N cluster is somewhat declined from the cage symmetry plane so that the overall symmetry of the molecule is C₁. We have symmetrized the structure and then considered all 47 nonequivalent carbon atoms of such rigorously C_s-symmetric $\text{Y}_3\text{N}@\text{C}_{84}$ as possible bonding sites for CH₃ and subsequently a dimer. Similar to $\text{Sc}_3\text{N}@\text{C}_{68}$ and $\text{Y}_3\text{N}@\text{C}_{78}$, the most stable isomers of $(\text{Y}_3\text{N}@\text{C}_{84})_2^{2-}$ found in the multistep approach are bonded via carbon atoms of adjacent pentagon pair (Figure 1f).

The carbon cage of $\text{Y}_3\text{N}@\text{C}_{86}$ has D₃(19) symmetry,^{39,40} which would be preserved for the whole molecule if the Y atoms would be coordinated to the centers of the hexagon. However, in the optimized structure of $\text{Y}_3\text{N}@\text{C}_{86}^-$, the cluster is significantly rotated, reducing the overall molecular symmetry to C₃. For the addition of the CH₃ group, we have considered two series of isomers, originating from D₃ and C₃ symmetric arrangements of Y_3N inside the cage, resulting in a total of 45 isomers of $\text{Y}_3\text{N}@\text{C}_{86}(\text{CH}_3)^-$. The multistep approach showed rather dense distribution of $(\text{Y}_3\text{N}@\text{C}_{86})_2^{2-}$ isomers with the four most stable structures (Figure 1l) in the range of only 6 kJ/mol at the PBE/TZ2P level. Of them one is bonded via PHHJ, and three others are bonded via THJ carbon atoms.

$\text{Y}_3\text{N}@\text{C}_{88}$ has a D₂(35)-symmetric carbon cage,⁴⁰ but the overall symmetry of optimized $\text{Y}_3\text{N}@\text{C}_{88}^-$ is close to C₂, which yields 44 isomers of $\text{Y}_3\text{N}@\text{C}_{88}(\text{CH}_3)^-$. Figure 1m shows two most stable isomers of $(\text{Y}_3\text{N}@\text{C}_{88})_2^{2-}$ found by the multistep approach within the energy range of 10.0 kJ/mol (PBE/TZ2P level).

General Remarks on the Molecular and Electronic Structures of $(\text{FLRN})_2^{2-}$ Dimers. Once the most stable isomers of single-bonded $(\text{FLRN})_2^{2-}$ dimers are localized, it is instructive to

Table 1. Bonding Sites, Inter-Cage Bond Lengths (d_{C-C}), HOMO-LUMO Gaps, Dimerization Energies (ΔE_{dim}), van der Waals (ΔE_{vdW}), and Solvation (ΔE_{solv}) Contributions to (ΔE_{dim}) as well as Coulomb Repulsion Energy in Dianionic Fullerene Dimers (FLRN) $_2^{2-}$ ^a

FLRN, no. of the isomer ^b	C-sp ³ ^c	d_{C-C} , Å	gap (eV)	ΔE_{dim} (gas)	gas+vdW	gas+vdW+solv	ΔE_{vdW}	ΔE_{solv}	E_{Coul}
C ₆₀	PHHJ	1.653	0.43	137	82	−53	−56	−135	115
C ₇₀	PHHJ	1.647	0.69	96	41	−85	−55	−126	103
C ₈₄ −I	PHHJ	1.675	0.15	134	67	−54	−67	−121	96
C ₈₄ −II	PHHJ	1.675	0.19	134	68	−51	−66	−119	96
Sc ₃ N@C ₆₈	P*HHJ	1.591	1.05	23	−41	−164	−64	−123	122
Sc ₃ N@C ₈₀	PHHJ	1.603	1.10	54	−8	−120	−62	−112	108
Sc ₃ N@C ₈₀ (CF ₃) ₂ −I	THJ	1.602	1.00	79	11	−91	−68	−102	105
Sc ₃ N@C ₈₀ (CF ₃) ₂ −II	PHHJ	1.605	0.84	89	22	−78	−67	−100	103
[5,6] Sc ₃ N@C ₈₀ (C ₃ H ₇ N)	THJ	1.616	1.10	88	−12	−92	−100	−80	108
[6,6] Sc ₃ N@C ₈₀ (C ₃ H ₇ N)−I	PHHJ	1.670	0.43	171	103	−10	−68	−113	108
[6,6] Sc ₃ N@C ₈₀ (C ₃ H ₇ N)−II	THJ	1.749	0.42	185	85	−4	−100	−89	104
Y ₃ N@C ₇₈	P*HHJ	1.580	0.82	56	−2	−126	−58	−123	113
Y ₃ N@C ₈₀ −I	THJ	1.601	1.11	63	6	−124	−57	−130	116
Y ₃ N@C ₈₀ −II	THJ	1.587	1.12	61	0	−121	−61	−121	115
[5,6] Y ₃ N@C ₈₀ (C ₃ H ₇ N)	THJ	1.615	0.98	77	−13	−98	−91	−84	113
[6,6] Y ₃ N@C ₈₀ (C ₃ H ₇ N)−I	THJ	1.594	1.07	93	23	−104	−70	−127	116
[6,6] Y ₃ N@C ₈₀ (C ₃ H ₇ N)−II	THJ	1.585	1.17	98	32	−99	−66	−131	115
Y ₃ N@C ₈₄	P*HHJ	1.582	0.78	47	−8	−125	−55	−117	109
Y ₃ N@C ₈₆ −I	THJ	1.605	0.91	77	9	−116	−68	−125	113
Y ₃ N@C ₈₆ −II	PHHJ	1.612	0.65	79	10	−103	−69	−113	109
Y ₃ N@C ₈₆ −III	THJ	1.606	1.08	80	20	−111	−60	−131	115
Y ₃ N@C ₈₆ −IV	THJ	1.609	1.13	82	14	−107	−67	−121	112
Y ₃ N@C ₈₈ −I	PHHJ	1.610	0.70	77	8	−103	−69	−111	107
Y ₃ N@C ₈₈ −II	THJ	1.608	1.07	83	10	−107	−72	−118	110
Y ₃ N@C ₈₈ −III	PHHJ	1.609	0.64	84	17	−106	−67	−123	107

^a All energy values are in kilojoules per mole. ^b See Figure 1 for designation of isomers. ^c PHHJ, pentagon–hexagon–hexagon junction; P*, pentagons in adjacent pentagon pairs; THJ, triple hexagon junction.

analyze the general trends in their molecular structures and compare empty fullerenes and NCFs. First of all, an important difference between these two kinds of fullerenes is that for NCFs there is no specific difference between the isomers bonded via THJ and PHHJ carbon atoms, whereas for the empty fullerenes bonding via THJ is strongly disfavored by the energy. Importantly, the THJ atoms forming intercage bonds in NCFs are usually close to the coordination sites of metal atom(s). In general, for the IPR cages, the atoms forming the most stable dimers are usually located close to the plane of the cluster and between the coordination sites of two metal atoms. The change of the role of THJs in endohedral metallofullerenes in comparison with empty fullerenes has already been pointed out in the studies of their addition reactions. First, multiple addition of single-bonded groups (CF₃, phenyl) to THJs has been reported for Sc₃N@C₈₀ and La@C₈₂−C_{3v}(7),^{34,35,41,42} whereas for empty higher fullerenes, the addition to THJs is usually avoided.^{33,43} Furthermore, for Sc₃N@C₈₀ and Y₃N@C₈₀, there is also an interesting parallel between dimerization and cycloaddition. For the cycloadducts such as fulleropyrrolidines, [5,6] isomers (both C-sp³ cage atoms are PHHJs) are strongly favored for Sc₃N@C₈₀, whereas [6,6] isomer with one C-sp³ THJ is equally stable for the Y₃N@C₈₀.⁴⁴ For the dimers, we have also found that switching from Sc to Y stabilizes the isomers of (M₃N@C₈₀)₂^{2−} bonded via THJs with respect to the PHHJ-bonded isomers.

The second important feature is that for the non-IPR NCFs, the most stable isomers are always bonded via peripheral atoms of adjacent pentagon units. This fact is also reflected in the already described chemical derivatives of non-IPR endohedral metallofullerenes.^{30–32,45}

For the derivatives of Sc₃N@C₈₀, the most electronically preferable positions for dimer formation are always close to the sp³ carbon atoms. However, this may result in difficulties for the dimer formation because of steric hindrances. As a result, the most stable isomers of (FLRN)₂^{2−} can be different from those of FLRN(CH₃)₂[−], as we have found in this work for Sc₃N@C₈₀−(CF₃)₂ and [6,6]−Sc₃N@C₈₀(C₃H₇N), and hence the intercage bonds in these dimers are relatively weak.

A characteristic feature of the dimeric structures is the length of the intercage bond. In dianionic dimers, these bonds are significantly elongated in comparison with the noncharged analogues (such as (C₅₉N)₂). Importantly, in the dimers of NCFs, the PBE/TZ2P optimized intercage bonds are ca. 0.04 to 0.05 Å shorter than those of empty fullerenes (Table 1). The only exclusion is the dimer of [6,6]−Sc₃N@C₈₀(C₃H₇N), which points to the unreleased strain in this structure, especially in the isomer II with the extremely long intercage bond of 1.749 Å.

It should also be noted that there is a certain correlation between the structures of the most stable isomers of the dimers and the spin density distribution in corresponding anion-radicals.

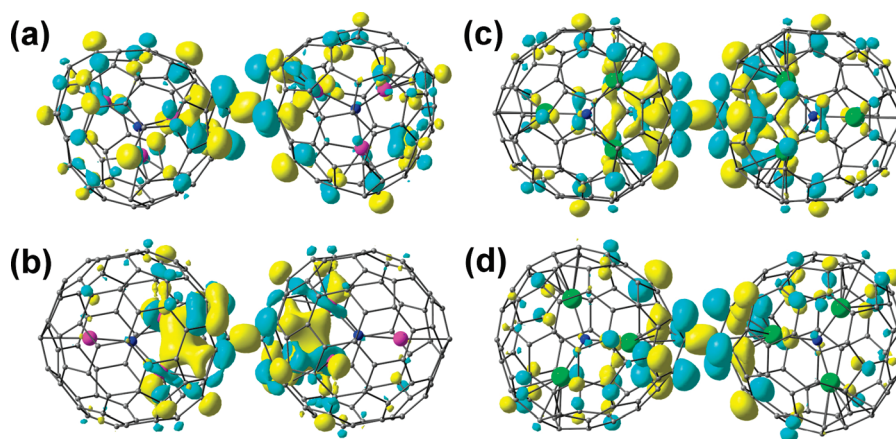


Figure 2. Highest occupied molecular orbitals of selected dianionic NCFs dimers: (a) $(\text{Sc}_3\text{N}@\text{C}_{68})_2^{2-}$, (b) $(\text{Sc}_3\text{N}@\text{C}_{80})_2^{2-}\text{-I}$, (c) $(\text{Y}_3\text{N}@\text{C}_{80})_2^{2-}\text{-I}$, and (d) $(\text{Y}_3\text{N}@\text{C}_{80})_2^{2-}\text{-II}$.

That is, carbon atoms with the highest spin populations in the latter usually serve as bonding sites in the most stable isomers of dimers, but this is not one-to-one correspondence in the sense that other factors (such as already discussed steric hindrance or local pyramidalization of the carbon cage) also play an important role.

One of the characteristic features of the electronic structure of single-bonded fullerene dimers is the specific molecular orbital (MO) with considerable intercage σ -bonding character.²⁹ In all studied NCF dimers, this type of MO is HOMO (representative examples are shown in Figure 2). At the same time, HOMO of the dimers also inherits a character of the SOMO of corresponding anion-radicals. For instance, the SOMO of $\text{Sc}_3\text{N}@\text{C}_{80}^-$ is largely localized on the Sc_3N cluster, and the same feature is seen for $(\text{Sc}_3\text{N}@\text{C}_{80})_2^{2-}$; in contrast, neither $\text{Y}_3\text{N}@\text{C}_{80}^-$ nor $(\text{Y}_3\text{N}@\text{C}_{80})_2^{2-}$ exhibits noticeable localization of SOMO/HOMO on the cluster.

Dimerization Energies. The search of the most stable isomers of each dimeric structure discussed above was crucial for the reliable analysis and comparison of the dimerization energies in the series of empty and endohedral fullerenes; all energies discussed below correspond to the most stable isomers of the dimers. It is not to be expected that absolute values of dimerization energies are predicted with high precision because of many factors such as basis set superposition error, empirical treatment of electron correlations at DFT level, basis set incompleteness error, and so on. However, the trends in the series of similar compounds are expected to be much more reliable. Table 1 lists dimerization energies for all types of fullerene structures studied in this work. At the PBE/TZ2P level in the gas phase (Table 1), dimeric states are much higher in energy than respective anion-radicals, which can be explained by the large effect of Coulomb repulsion between charged monomers. It can already be seen at this level that dianionic dimers of NCFs are much more stable than those of empty fullerenes. (The only exception is $[6,6]\text{-Sc}_3\text{N}@\text{C}_{80}^-$ ($\text{C}_3\text{H}_7\text{N}$), whose dimerization energy is closer to that of empty fullerenes.)

To analyze the role of the endohedral clusters in Coulomb repulsion, we have roughly estimated Coulomb term (E_{Coul}) as a sum of pairwise point charge interactions using Hirschfeld atomic charges computed at the PBE/TZ2P level and summing up only the interaction between the atoms from different monomeric units. (In ref 29, we used this approach to estimate E_{Coul} in $(\text{C}_{70})_2^{2+}$.) For all dianionic fullerene dimers, E_{Coul}

found this way is close to 100–110 kJ/mol. For empty fullerenes, the values are decreasing from 115 kJ/mol for $(\text{C}_{60})_2^{2-}$ to 96 kJ/mol for $(\text{C}_{84})_2^{2-}$. For the dimer of $\text{Sc}_3\text{N}@\text{C}_{80}$, this approach gives $E_{\text{Coul}} = 108$ kJ/mol, in which the cage–cage repulsion term is as large as 385 kJ/mol. Taking into account the electron transfer to the carbon cage and its negative charge in the neutral NCFs, considerable increase in the cage–cage repulsion in NCF dimers in comparison with the dimers of empty fullerenes is clearly justified. However, this large repulsive term is almost completely canceled by the cluster–(other cage) interactions, which yield -363 kJ/mol in $(\text{Sc}_3\text{N}@\text{C}_{80})_2^{2-}$. Finally, cluster–cluster interactions are repulsive and add 86 kJ/mol to E_{Coul} . This example clearly shows that Coulomb interactions between the cluster in one monomeric unit and the cage in another unit play an important role in the stabilization of the NCF dimers. Similar E_{Coul} values are obtained for dimers of all other NCFs, and in all cases, large cage–cage repulsion is compensated by rather strong interaction between the cluster and the cage of other monomeric unit (see Supporting Information for more details) yielding total E_{Coul} values close to those of empty fullerenes. Thus, it can be concluded that increased stability of $(\text{NCF})_2^{2-}$ dimers in comparison with those of empty fullerenes is the result of a stronger covalent bonding between the cages and is not due to the specific charge distribution in endohedral metallofullerenes that might reduce Coulomb repulsion. This conclusion agrees well with shorter intercage bonds found for NCFs (Table 1; see Supporting Information for correlation between intercage bond lengths and dimerization energies).

In addition to Coulomb repulsion, van der Waals (vdW) interactions can be of high importance for the stabilization of dimeric structures, but they are poorly described by the standard DFT approaches. To overcome this shortcoming, an empirical vdW correction to PBE values was estimated with the use of Grimme's DFT-D approach^{46,47} (Table 1). The vdW term strongly stabilizes the dimers changing the dimerization energies by 60–70 kJ/mol (up to 100 kJ/mol for the dimers of pyrrolidine adducts). As a result, at the PBE-D level, many NCFs are predicted to have bounded dimeric states already in the gas phase despite the Coulomb repulsion. (But the ground state of the anion-radicals of empty fullerenes is still unbound.) The vdW corrections for different isomers vary in most cases within the range of ca. 10 kJ/mol, and thus they can slightly change stability

order of the isomers. There is no specific difference in ΔE_{vdW} term for empty fullerenes and nonderivatized NCFs.

Finally, electrochemical studies are performed in solution, and solvation can drastically change dimerization energies. To analyze the effect of this factor, we have evaluated solvation energies at the PBE/(STO-DZVP) level using the COSMO-RS⁴⁸ model implemented in ADF. In all cases, solvation substantially stabilizes dimers with respect to the monoanions (Table 1). As a result, all dimers are energetically more preferable in solution than respective monomers. The stabilization effect is gradually decreasing with the size of the fullerene from -135 kJ/mol for C_{60} to -111 kJ/mol for $\text{Y}_3\text{N@C}_{88}$, which can be rationalized by recalling the $1/R$ term in Born's theory of solvation. The value for isomers can vary within 10 – 15 kJ/mol, changing in some cases the stability order of the isomers in comparison with the gas phase. As with the ΔE_{vdW} term, there is no special difference in ΔE_{solv} values for empty fullerenes and NCFs.

Among the empty fullerenes, the most stable is the dimer of C_{70}^{2-} . Its dimerization energy in solution is close to that of $\text{Sc}_3\text{N@C}_{80}(\text{CF}_3)_2^-$ and $[\text{5,6}]\text{-Sc}_3\text{N@C}_{80}(\text{C}_3\text{H}_7\text{N})^-$, which are among the least stable dimers in the whole NCF series and exhibit reversible reductions. The next structure in the order of dimer stability is $(\text{Y}_3\text{N@C}_{88})_2^{2-}$. Note that $\text{M}_3\text{N@C}_{88}$ also exhibits reversible reductions. All other nonderivatized NCFs form more stable dimers, and this fact agrees well with irreversible reduction steps found for them in electrochemical studies. Importantly, our calculations also reveal the dramatic difference in the dimerization energies of $[\text{6,6}]\text{-Sc}_3\text{N@C}_{80}(\text{C}_3\text{H}_7\text{N})^-$, which forms the least stable dianionic dimer in the whole series, and $[\text{6,6}]\text{-Y}_3\text{N@C}_{80}(\text{C}_3\text{H}_7\text{N})^-$, whose dimerization energy in oDCB is ca. 100 kJ/mol higher. This fact also agrees with different reduction behavior of $[\text{6,6}]$ adducts of $\text{Sc}_3\text{N@C}_{80}$, on the one hand, and all other $\text{M}_3\text{N@C}_{80}$, on the other hand.²⁵

Concluding Remarks. In this work, using DFT theory, we have studied in detail dimerization of the anion-radical of NCFs to find if formation of the dimers can be an explanation of the irreversible reduction steps exhibiting by these compounds. In the first stage, we have found stable dimers and described the special features in the dimer formation for NCFs. In sharp contrast with empty fullerenes, dianionic dimers of NCFs bonded via carbon atoms on triple-hexagon junctions are equally as stable as those bonded via carbon atoms in pentagons. For non-IPR NCFs, the most stable dimers are always bonded via peripheral carbon atoms of adjacent pentagon pairs.

When van der Waals and solvation terms are taken into account, the dianionic dimers of all nonderivatized NCFs are significantly more stable than the dimers of empty fullerenes. The least stable dimer is found for $\text{Y}_3\text{N@C}_{88}$, and it is the only non-Sc $\text{M}_3\text{N@C}_{2n}$ ($2n = 78$ – 88) NCF exhibiting reversible reduction. The study has also shown that the dimers of $\text{Sc}_3\text{N@C}_{80}$ derivatives, such as $\text{Sc}_3\text{N@C}_{80}(\text{CF}_3)_2$ or pyrrolidine cycloadducts, are significantly less stable than the dimers of nonderivatized NCFs. From the electronic point of view, the most preferable bonding sites in derivatives of NCFs are located close to the derivatized fragments. However, the formation of dimers via these bonding sites is either impossible or leads to the unstable dimers because of the steric hindrances. The low stability of such dimers agrees well with reversible reductions exhibited by these compounds. Although entropy or kinetic factors have not been considered in this work, a reasonable correlation between the stability of the dianionic dimers and the reversibility of electrochemical reduction of NCFs shows that reversible

formation of the dimers from anion radicals is a likely an explanation of the irreversible electrochemical behavior of NCFs. In this regard, reversible reduction of $\text{TiSc}_2\text{N@C}_{80}$ reported by us recently⁴⁹ can be explained by the fact that its monoanion is not a radical and hence is not prone to dimerization.

COMPUTATIONAL DETAILS

Optimization of the molecular structure of all species reported in this work was performed using PBE functional⁵⁰ and TZ2P-quality basis set (full-electron $\{6,3,2\}/\{11s,6p,2d\}$ for C and N atoms and SBK-type effective core potential for Sc and Y atoms with $\{5,5,4\}/\{9s,9p,8d\}$ valence part) implemented in the PRIR-ODA package.^{51,52} Preliminary screening of the isomers was performed using DZ-quality basis sets $\{2\}/\{4s\}$ and $\{3,2\}/\{7s,4p\}$ for H and C atoms, respectively, and DZVP-quality $\Lambda 1$ basis set⁵³ for Sc, Y, and endohedral nitrogen. The code employed expansion of the electron density in an auxiliary basis set to accelerate evaluation of the Coulomb and exchange-correlation terms.⁵² van der Waals corrections were computed using Grimme's DFT-D method,^{46,47} as implemented in ORCA.⁵⁴ Testing calculations have shown that the use of vdW corrections in the course of optimization slightly shortened the intercage bond length. Solvation energies were computed at the PBE/(STO-DZVP⁵⁵) level using COSMO-RS approach⁴⁸ implemented in ADF 2010.02.^{56,57} Computations were performed for *o*-dichlorobenzene solvent; similar values (in most cases within 10 kJ/mol) were also obtained for CH_2Cl_2 . The increase in the basis set to STO-TZ2P changed the values by <5 kJ/mol.

ASSOCIATED CONTENT

S Supporting Information. Correlation of stability between isomers of $\text{FLRN}(\text{CH}_3)^-$ and $(\text{FLRN})_2^{2-}$ and additional computational data; Cartesian coordinates. This material is available free of charge via the Internet at <http://pubs.acs.org>.

AUTHOR INFORMATION

Corresponding Author

*E-mail: a.popov@ifw-dresden.de.

ACKNOWLEDGMENT

AvH Foundation and Erasmus Mundus programme External Co-operation (EM ECW-L04 TUD 08-11) are acknowledged for financial support to A.A.P. and S.M.A., respectively. G.C. thanks World Class University program sponsored by the South Korean Ministry of Education, Science, and Technology Program, project R31-2008-000-10100-0. Computational Center in Moscow State University is acknowledged for computer time on "Chebyshev SKIF-MSU" supercomputer. We also thank the Center for Information Services and High Performance Computing (ZIH) at TU Dresden for computational time on its clusters. Technical assistance of U. Nitzsche with local computer resources at IFW Dresden is highly appreciated.

REFERENCES

- (1) Dunsch, L.; Yang, S. Metal Nitride Cluster Fullerenes: Their Current State and Future Prospects. *Small* **2007**, *3*, 1298–1320.
- (2) Chaur, M. N.; Melin, F.; Ortiz, A. L.; Echegoyen, L. Chemical, Electrochemical, and Structural Properties of Endohedral Metallofullerenes. *Angew. Chem., Int. Ed.* **2009**, *48*, 7514–7538.

- (3) Feng, M.; Zhao, J.; Huang, T.; Zhu, X.; Petek, H. The Electronic Properties of Supramolecular States of Hollow Molecules. *Acc. Chem. Res.* **2011**, *44*, 360–368.
- (4) Ioffe, I. N.; Ievlev, A. S.; Boltalina, O. V.; Sidorov, L. N.; Dorn, H. C.; Stevenson, S.; Rice, G. Electron Affinity of Some Trimetallic Nitride and Conventional Metallofullerenes. *Int. J. Mass Spectrom.* **2002**, *213*, 183–189.
- (5) Pinzyn, J. R.; Plonska-Brzezinska, M. E.; Cardona, C. M.; Athans, A. J.; Gayathri, S. S.; Guldi, D. M.; Herranz, M. A.; Martin, N.; Torres, T.; Echegoyen, L. $\text{Sc}_3\text{N}@C_{80}$ -Ferrocene Electron-Donor/Acceptor Conjugates as Promising Materials for Photovoltaic Applications. *Angew. Chem., Int. Ed.* **2008**, *47*, 4173–4176.
- (6) Pinzon, J. R.; Gasca, D. C.; Sankaranarayanan, S. G.; Bottari, G.; Torres, T.; Guldi, D. M.; Echegoyen, L. Photoinduced Charge Transfer and Electrochemical Properties of Triphenylamine $I_h\text{-Sc}_3\text{N}@C_{80}$ Donor-Acceptor Conjugates. *J. Am. Chem. Soc.* **2009**, *131*, 7727–7734.
- (7) Pinzyn, J. R.; Cardona, C. M.; Herranz, M. A.; Plonska-Brzezinska, M. E.; Palkar, A.; Athans, A. J.; Martin, N.; Rodriguez-Fortea, A.; Poblet, J. M.; Bottari, G.; et al. Metal Nitride Cluster Fullerene $\text{M}_3\text{N}@C_{80}$ ($\text{M} = \text{Y}, \text{Sc}$) Based Dyads: Synthesis, and Electrochemical, Theoretical and Photophysical Studies. *Chem.—Eur. J.* **2009**, *15*, 864–877.
- (8) Ross, R. B.; Cardona, C. M.; Guldi, D. M.; Sankaranarayanan, S. G.; Reese, M. O.; Kopidakis, N.; Peet, J.; Walker, B.; Bazan, G. C.; Van Keuren, E.; et al. Endohedral Fullerenes for Organic Photovoltaic Devices. *Nat. Mater.* **2009**, *8*, 208–212.
- (9) Elliott, B.; Yu, L.; Echegoyen, L. A Simple Isomeric Separation of D_{5h} and I_h $\text{Sc}_3\text{N}@C_{80}$ by Selective Chemical Oxidation. *J. Am. Chem. Soc.* **2005**, *127*, 10885–10888.
- (10) Cardona, C. M.; Elliott, B.; Echegoyen, L. Unexpected Chemical and Electrochemical Properties of $\text{M}_3\text{N}@C_{80}$ ($\text{M} = \text{Sc}, \text{Y}, \text{Er}$). *J. Am. Chem. Soc.* **2006**, *128*, 6480–6485.
- (11) Plonska-Brzezinska, M. E.; Athans, A. J.; Phillips, J. P.; Stevenson, S.; Echegoyen, L. A Reinvestigation of the Electrochemical Behavior of $\text{Sc}_3\text{N}@C_{80}$. *J. Electroanal. Chem.* **2008**, *614*, 171–174.
- (12) Chaur, M. N.; Aparicio-Angles, X.; Mercado, B. Q.; Elliott, B.; Rodriguez-Fortea, A.; Clotet, A.; Olmstead, M. M.; Balch, A. L.; Poblet, J. M.; Echegoyen, L. Structural and Electrochemical Property Correlations of Metallic Nitride Endohedral Metallofullerenes. *J. Phys. Chem. C* **2010**, *114*, 13003–13009.
- (13) Chaur, M. N.; Athans, A. J.; Echegoyen, L. Metallic Nitride Endohedral Fullerenes: Synthesis and Electrochemical Properties. *Tetrahedron* **2008**, *64*, 11387–11393.
- (14) Yang, S. F.; Zalibera, M.; Rapta, P.; Dunsch, L. Charge-Induced Reversible Rearrangement of Endohedral Fullerenes: Electrochemistry of Tridysprosium Nitride Clusterfullerenes $\text{Dy}_3\text{N}@C_{2n}$ ($2n = 78, 80$). *Chem.—Eur. J.* **2006**, *12*, 7848–7855.
- (15) Rapta, P.; Popov, A. A.; Yang, S. F.; Dunsch, L. The Charged States of $\text{Sc}_3\text{N}@C_{68}$: An in Situ Spectroelectrochemical Study of the Radical Cation and Radical Anion of a Non-IPR Fullerene. *J. Phys. Chem. A* **2008**, *112*, 5858–5865.
- (16) Tarabek, J.; Yang, S.; Dunsch, L. Redox Properties of Mixed Lutetium/Yttrium Nitride Clusterfullerenes: Endohedral $\text{Lu}_x\text{Y}_{3-x}\text{N}@C_{80}(\text{I})$ ($x = 0–3$) Compounds. *ChemPhysChem* **2009**, *10*, 1037–1043.
- (17) Chaur, M. N.; Melin, F.; Elliott, B.; Athans, A. J.; Walker, K.; Holloway, B. C.; Echegoyen, L. $\text{Gd}_3\text{N}@C_{2n}$ ($n = 40, 42$, and 44): Remarkably Low HOMO-LUMO Gap and Unusual Electrochemical Reversibility of $\text{Gd}_3\text{N}@C_{88}$. *J. Am. Chem. Soc.* **2007**, *129*, 14826–14829.
- (18) Cai, T.; Xu, L.; Shu, C.; Champion, H. A.; Reid, J. E.; Anklin, C.; Anderson, M. R.; Gibson, H. W.; Dorn, H. C. Selective Formation of a Symmetric $\text{Sc}_3\text{N}@C_{78}$ Bisadduct: Adduct Docking Controlled by an Internal Trimetallic Nitride Cluster. *J. Am. Chem. Soc.* **2008**, *130*, 2136–2137.
- (19) Popov, A. A.; Dunsch, L. Hindered Cluster Rotation and ^{45}Sc Hyperfine Splitting Constant in Distonoid Anion Radical $\text{Sc}_3\text{N}@C_{80}$, and Spatial Spin Charge Separation as a General Principle for Anions of Endohedral Fullerenes with Metal-Localized Lowest Unoccupied Molecular Orbitals. *J. Am. Chem. Soc.* **2008**, *130*, 17726–17742.
- (20) Zhang, L.; Popov, A. A.; Yang, S.; Klod, S.; Rapta, P.; Dunsch, L. An Endohedral Redox System in a Fullerene Cage: The Ce Based Mixed Cluster Fullerene $\text{Lu}_2\text{CeN}@C_{80}$. *Phys. Chem. Chem. Phys.* **2010**, *12*, 7840–7847.
- (21) Valencia, R.; Rodriguez-Fortea, A.; Clotet, A.; de Graaf, C.; Chaur, M. N.; Echegoyen, L.; Poblet, J. M. Electronic Structure and Redox Properties of Metal Nitride Endohedral Fullerenes $\text{M}_3\text{N}@C_{2n}$ ($\text{M} = \text{Sc}, \text{Y}, \text{La}$, and Gd ; $2n = 80, 84, 88, 92, 96$). *Chem.—Eur. J.* **2009**, *15*, 10997–11009.
- (22) Chaur, M. N.; Valencia, R.; Rodriguez-Fortea, A.; Poblet, J. M.; Echegoyen, L. Trimetallic Nitride Endohedral Fullerenes: Experimental and Theoretical Evidence for the $\text{M}_3\text{N}^{6+}@C_{2n}^{6-}$ Model. *Angew. Chem., Int. Ed.* **2009**, *48*, 1425–1428.
- (23) Popov, A. A.; Shustova, N. B.; Svitova, A. L.; Mackey, M. A.; Coumbe, C. E.; Phillips, J. P.; Stevenson, S.; Strauss, S. H.; Boltalina, O. V.; Dunsch, L. Redox-Tuning Endohedral Fullerene Spin States: From the Dication to the Trianion Radical of $\text{Sc}_3\text{N}@C_{80}(\text{CF}_3)_2$ in Five Reversible Single-Electron Steps. *Chem.—Eur. J.* **2010**, *16*, 4721–4724.
- (24) Echegoyen, L.; Chancellor, C. J.; Cardona, C. M.; Elliott, B.; Rivera, J.; Olmstead, M. M.; Balch, A. L. X-Ray Crystallographic and EPR Spectroscopic Characterization of a Pyrrolidine Adduct of $\text{Y}_3\text{N}@C_{80}$. *Chem. Commun.* **2006**, 2653–2655.
- (25) Chen, N.; Pinzón, J. R.; Echegoyen, L. Influence of the Encapsulated Clusters on the Electrochemical Behaviour of Endohedral Fullerene Derivatives: Comparative Study of *N*-Tritylpyrrolidino Derivatives of $\text{Sc}_3\text{N}@I_h\text{-C}_{80}$ and $\text{Lu}_3\text{N}@I_h\text{-C}_{80}$. *ChemPhysChem* **2011**, *12*, 1422–1425.
- (26) Li, F.-F.; Pinzon, J. R.; Mercado, B. Q.; Olmstead, M. M.; Balch, A. L.; Echegoyen, L. $[2 + 2]$ Cycloaddition Reaction to $\text{Sc}_3\text{N}@I_h\text{-C}_{80}$. The Formation of Very Stable $[5,6]$ - and $[6,6]$ -Adducts. *J. Am. Chem. Soc.* **2011**, *133*, 1563–1571.
- (27) Konarev, D. V.; Khasanov, S. S.; Otsuka, A.; Saito, G.; Lyubovskaya, R. N. Formation of Antiferromagnetically Coupled C_{60}^{0-} and Diamagnetic $(\text{C}_{70}^{0-})_2$ Dimers in Ionic Complexes of Fullerenes with $(\text{MDABCO}^+)_2 \cdot \text{M}^{\text{II}}\text{TPP}$ ($\text{M} = \text{Zn}, \text{Co}, \text{Mn}$, and Fe) Assemblies. *Inorg. Chem.* **2007**, *46*, 2261–2271.
- (28) Konarev, D. V.; Lyubovskaya, R. N.; Khasanov, S. S.; Otsuka, A.; Saito, G. Formation and Properties of $(\text{C}_{60}^{0-})_2$ Dimers of Fullerenes Bonded by One and Two Sigma-Bonds in Ionic Complexes. *Mol. Cryst. Liq. Cryst.* **2007**, *468*, 579–589.
- (29) Popov, A. A.; Burtsev, A. V.; Senyavin, V. M.; Dunsch, L.; Troyanov, S. I. Spectroscopic and Theoretical Study of the Dimeric Dicationic Fullerene Complex $[(\text{C}_{70})_2]^{2+}(\text{Ti}_3\text{Cl}_{13})^{2-}$. *J. Phys. Chem. A* **2008**, *113*, 263–272.
- (30) Lu, X.; Nikawa, H.; Nakahodo, T.; Tsuchiya, T.; Ishitsuka, M. O.; Maeda, Y.; Akasaka, T.; Toki, M.; Sawa, H.; Slanina, Z.; Mizorogi, N.; Nagase, S. Chemical Understanding of a Non-IPR Metallofullerene: Stabilization of Encaged Metals on Fused-Pentagon Bonds in $\text{La}_2@C_{72}$. *J. Am. Chem. Soc.* **2008**, *130*, 9129–9136.
- (31) Lu, X.; Nikawa, H.; Tsuchiya, T.; Maeda, Y.; Ishitsuka, M. O.; Akasaka, T.; Toki, M.; Sawa, H.; Slanina, Z.; Mizorogi, N.; Nagase, S. Biscarbene Adducts of Non-IPR $\text{La}_2@C_{72}$: Localization of High Reactivity around Fused-Pentagons and toward Controllable Tuning of Electrochemical Properties of Metallofullerenes. *Angew. Chem., Int. Ed.* **2008**, *47*, 8642–8645.
- (32) Cai, T.; Xu, L.; Shu, C.; Reid, J. E.; Gibson, H. W.; Dorn, H. C. Synthesis and Characterization of a Non-IPR Fullerene Derivative: $\text{Sc}_3\text{N}@C_{68}[\text{C}(\text{COOC}_2\text{H}_5)_2]$. *J. Phys. Chem. C* **2008**, *112*, 19203–19208.
- (33) Shustova, N. B.; Kuvychko, I. V.; Bolskar, R. D.; Seppelt, K.; Strauss, S. H.; Popov, A. A.; Boltalina, O. V. Trifluoromethyl Derivatives of Insoluble Small-HOMO-LUMO-Gap Hollow Higher Fullerenes. NMR and DFT Structure Elucidation of $\text{C}_{2-}(\text{C}_{74}\text{-D}_{3h})(\text{CF}_3)_{12}$, $\text{C}_{2-}(\text{C}_{76}\text{-T}_d)(\text{CF}_3)_{12}$, $\text{C}_{2-}(\text{C}_{78}\text{-D}_{3h})(\text{CF}_3)_{12}$, $\text{C}_{2-}(\text{C}_{80}\text{-C}_{2v}(5))(\text{CF}_3)_{12}$, and $\text{C}_{2-}(\text{C}_{82}\text{-C}_{2v}(5))(\text{CF}_3)_{12}$. *J. Am. Chem. Soc.* **2006**, *128*, 15793–15798.
- (34) Shustova, N. B.; Chen, Y.-S.; Mackey, M. A.; Coumbe, C. E.; Phillips, J. P.; Stevenson, S.; Popov, A. A.; Boltalina, O. V.; Strauss, S. H.

Sc₃N@C₈₀-I_h(7))(CF₃)₁₄ and Sc₃N@C₈₀-I_h(7))(CF₃)₁₆. Endohedral Metallofullerene Derivatives with Exohedral Addends on Four and Eight Triple-Hexagon Junctions. Does the Sc₃N Cluster Control the Addition Pattern or Vice Versa? *J. Am. Chem. Soc.* **2009**, *131*, 17630–17637.

(35) Shustova, N. B.; Peryshkov, D. V.; Kuvychko, I. V.; Chen, Y.-S.; Mackey, M. A.; Coumbe, C. E.; Heaps, D. T.; Confait, B. S.; Heine, T.; Phillips, J. P.; et al. Poly(Perfluoroalkylation) of Metallic Nitride Fullerenes Reveals Addition-Pattern Guidelines: Synthesis and Characterization of a Family of Sc₃N@C₈₀(CF₃)_n (n = 2–16) and Their Radical Anions. *J. Am. Chem. Soc.* **2011**, *133*, 2672–2690.

(36) Shustova, N. B.; Popov, A. A.; Mackey, M. A.; Coumbe, C. E.; Phillips, J. P.; Stevenson, S.; Strauss, S. H.; Boltalina, O. V. Radical Trifluoromethylation of Sc₃N@C₈₀. *J. Am. Chem. Soc.* **2007**, *129*, 11676–11677.

(37) Popov, A. A.; Krause, M.; Yang, S. F.; Wong, J.; Dunsch, L. C₇₈ Cage Isomerism Defined by Trimetallic Nitride Cluster Size: A Computational and Vibrational Spectroscopic Study. *J. Phys. Chem. B* **2007**, *111*, 3363–3369.

(38) Beavers, C. M.; Zuo, T. M.; Duchamp, J. C.; Harich, K.; Dorn, H. C.; Olmstead, M. M.; Balch, A. L. Tb₃N@C₈₄: An Improbable, Egg-Shaped Endohedral Fullerene That Violates the Isolated Pentagon Rule. *J. Am. Chem. Soc.* **2006**, *128*, 11352–11353.

(39) Fu, W.; Xu, L.; Azurmendi, H.; Ge, J.; Fuhrer, T.; Zuo, T.; Reid, J.; Shu, C.; Harich, K.; Dorn, H. C. ⁸⁹Y and ¹³C NMR Cluster and Carbon Cage Studies of an Yttrium Metallofullerene Family, Y₃N@C_{2n} (n = 40–43). *J. Am. Chem. Soc.* **2009**, *131*, 11762–11769.

(40) Zuo, T. M.; Beavers, C. M.; Duchamp, J. C.; Campbell, A.; Dorn, H. C.; Olmstead, M. M.; Balch, A. L. Isolation and Structural Characterization of a Family of Endohedral Fullerenes Including the Large, Chiral Cage Fullerenes Tb₃N@C₈₈ and Tb₃N@C₈₆ as Well as the I_h and D_{5h} Isomers of Tb₃N@C₈₀. *J. Am. Chem. Soc.* **2007**, *129*, 2035–2043.

(41) Yang, S.; Chen, C.; Lansikh, M. A.; Tamm, N. B.; Kemnitz, E.; Troyanov, S. I. New Isomers of Trifluoromethylated Derivatives of Metal Nitride Cluster Fullerene: Sc₃N@C₈₀(CF₃)_n (n = 14 and 16). *Chem. –Asian J.* **2011**, *6*, 505–509.

(42) Akasaka, T.; Lu, X.; Kuga, H.; Nikawa, H.; Mizorogi, N.; Slanina, Z.; Tsuchiya, T.; Yoza, K.; Nagase, S. Dichlorophenyl Derivatives of La@C_{3v}(7)-C₈₂: Endohedral Metal Induced Localization of Pyramidalization and Spin on a Triple-Hexagon Junction. *Angew. Chem., Int. Ed.* **2011**, *49*, 9715–9719.

(43) Kareev, I. E.; Popov, A. A.; Kuvychko, I. V.; Shustova, N. B.; Lebedkin, S. F.; Bubnov, V. P.; Anderson, O. P.; Seppelt, K.; Strauss, S. H.; Boltalina, O. V. Synthesis and X-ray or NMR/DFT Structure Elucidation of Twenty-One New Trifluoromethyl Derivatives of Soluble Cage Isomers of C₇₆, C₇₈, C₈₄, and C₉₀. *J. Am. Chem. Soc.* **2008**, *130*, 13471–13489.

(44) Rodriguez-Forte, A.; Campanera, J. M.; Cardona, C. M.; Echegoyen, L.; Poblet, J. M. Dancing on a Fullerene Surface: Isomerization of Y₃N@N-Ethylpyrrolidino-C₈₀ from the 6,6 to the 5,6 Regioisomer. *Angew. Chem., Int. Ed.* **2006**, *45*, 8176–8180.

(45) Alegret, N.; Chaur, M. N.; Santos, E.; Rodriguez-Forte, A.; Echegoyen, L.; Poblet, J. M. Bingel-Hirsch Reactions on Non-IPR Gd₃N@C_{2n} (2n = 82 and 84). *J. Org. Chem.* **2010**, *75*, 8299–8302.

(46) Grimme, S. Accurate Description of Van Der Waals Complexes by Density Functional Theory Including Empirical Corrections. *J. Comput. Chem.* **2004**, *25*, 1463–1473.

(47) Grimme, S. Semiempirical GGA-Type Density Functional Constructed with a Long-Range Dispersion Correction. *J. Comput. Chem.* **2006**, *27*, 1787–1799.

(48) Pye, C. C.; Ziegler, T.; van Lenthe, E.; Louwen, J. N. An Implementation of the Conductor-Like Screening Model of Solvation within the Amsterdam Density Functional Package - Part II. COSMO for Real Solvents. *Can. J. Chem.* **2009**, *87*, 790–797.

(49) Popov, A. A.; Chen, C.; Yang, S.; Lipps, F.; Dunsch, L. Spin-Flow Vibrational Spectroscopy of Molecules with Flexible Spin Density: Electrochemistry, ESR, Cluster and Spin Dynamics, and Bonding in TiSc₂N@C₈₀. *ACS Nano* **2010**, *4*, 4857–4871.

(50) Perdew, J. P.; Burke, K.; Ernzerhof, M. Generalized Gradient Approximation Made Simple. *Phys. Rev. Lett.* **1996**, *77*, 3865–3868.

(51) Laikov, D. N.; Ustynuk, Y. A. Priroda-04: A Quantum-Chemical Program Suite. New Possibilities in the Study of Molecular Systems with the Application of Parallel Computing. *Russ. Chem. Bull.* **2005**, *54*, 820–826.

(52) Laikov, D. N. Fast Evaluation of Density Functional Exchange-Correlation Terms Using the Expansion of the Electron Density in Auxiliary Basis Sets. *Chem. Phys. Lett.* **1997**, *281*, 151–156.

(53) Laikov, D. N. A New Class of Atomic Basis Functions for Accurate Electronic Structure Calculations of Molecules. *Chem. Phys. Lett.* **2005**, *416*, 116–120.

(54) Neese, F. *Orca, An Ab Initio, Density Functional and Semiempirical Program Package*, version 2.8; Institute for Physical and Theoretical Chemistry: Bonn, Germany, 2010.

(55) Van Lenthe, E.; Baerends, E. J. Optimized Slater-Type Basis Sets for the Elements 1–118. *J. Comput. Chem.* **2003**, *24*, 1142–1156.

(56) *ADF2010*; SCM, Theoretical Chemistry, Vrije Universiteit: Amsterdam, The Netherlands, 2010. <http://www.scm.com>.

(57) te Velde, G.; Bickelhaupt, F. M.; Baerends, E. J.; Fonseca Guerra, C.; van Gisbergen, S. J. A.; Snijders, J. G.; Ziegler, T. Chemistry with ADF. *J. Comput. Chem.* **2001**, *22*, 931–967.